Journal of Medicinal Chemistry

pubs.acs.org/jmc



Article

# Discovery of Thermal Sensitizers That Inhibit Heat-Induced SAFB Granule Formation

Yuji Furutani, Natsuki Shimasaki, Riko Yamada, Takashi Ohtsuki, and Kazunori Watanabe*

Cite This: J. Med. Chem. 2026, 69, 5944−5955

Read Online

ACCESS | Metrics & More | Article Recommendations | Supporting Information

**ABSTRACT:** Hyperthermia is a minimally invasive cancer treatment based on heat stress-induced apoptosis. Its therapeutic efficacy, however, is often limited by tumor heterogeneity and acquired thermotolerance. Therefore, combination strategies involving hyperthermia and chemotherapy have been developed to enhance the therapeutic efficacy. Previously, we showed that SB366791 enhanced heat-induced apoptosis by inhibiting heat stress-induced scaffold attachment factor B (SAFB) granule formation, although its proapoptotic activity was insufficient. Therefore, we screened to identify novel compounds that enhance heat-induced apoptosis by suppressing SAFB granule formation. We identified four hit compounds that inhibited SAFB granule formation, all exhibiting thermal enhancement ratios > 1.0—that significantly enhanced heat-induced apoptosis efficiency. Additionally, the tumor volume in mice treated with a combination of Z19024498 and hyperthermia was significantly smaller than that in mice treated with hyperthermia or Z19024498. These results indicate that the identified compounds, specifically Z19024498, have potential as thermal sensitizers for hyperthermia therapy.

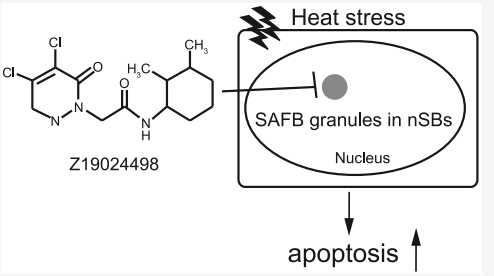




## INTRODUCTION

Hyperthermic therapy is a minimally invasive cancer treatment based on heat stress-induced apoptosis. Hyperthermia-induced apoptotic cell death increases at 39−42 °C and peaks at 43 °C and higher.[1−3] However, hyperthermia alone presents several challenges—it cannot effectively eradicate cancer cells because of tumor heterogeneity and acquired thermal resistance through cellular thermal responses.[4] To overcome these limitations, combination therapies involving hyperthermia and chemotherapeutic drugs, such as cisplatin and 5-fluorouracil (5-FU) have been developed.[5,6] These combination treatments that exhibit synergistic effects achieve enhanced anticancer effects at low doses of therapeutic drugs. Additionally, the combination treatments have been applied to various cancer types.[7] Therefore, chemotherapeutic drugs that enhance the effects of hyperthermia are termed thermal sensitizers.

Despite the promise of combined therapy, its efficacy remains limited because of the upregulation of chaperone proteins associated with thermal resistance. Because heat shock proteins (HSPs), a subgroup of chaperone proteins, refold unfolded and inactivated proteins, HSP inhibitors, such as HSP90 inhibitors (ganetespib and 17-dimethylaminoethylamino-17-demethoxygeldanamycin [17-DMAG]) and HSP70 inhibitors (pifithrin-$\mu$ and quercetin), enhance heat stress-induced cell death in vitro and/or suppress tumor growth in vivo.[8−11] These reports indicate that HSP inhibitors can potentiate hyperthermia-mediated cancer therapies. However, owing to their high toxicity, clinical trials involving ganetespib and 17-DMAG have been suspended,[12] leaving these inhibitors in the early stages of therapeutic development.

One such thermal response is the formation of stress-induced granules. These granules are classified into stress granules (SGs)—formed in the cytoplasm, and nuclear stress bodies (nSBs)—formed in the nucleus.[13,14] These granules are membraneless structures formed through liquid−liquid phase separation.[15,16] Although SGs are commonly observed in stress-exposed eukaryotic cells, nSBs are uniquely observed in primates.[13]

nSBs consist of 141 RNA-binding proteins and a few noncoding RNAs.[17] Their major components are heat shock transcription factor 1 (HSF1),[18] scaffold attachment factor B (SAFB),[19] satellite III long noncoding RNA (Sat III RNA),[20] and initiator and elongator tRNAs.[21] Heat stress-induced apoptosis was enhanced in the presence of SB366791, which inhibits the formation of SAFB granules, and 0.1% 2,5-hexanediol (2,5-HD), which inhibits the formation of both HSF1 and SAFB granules.[16] It has been indicated that these compounds act by inhibiting HSP70 upregulation during recovery from heat stress. These findings indicate that inhibiting HSF1 and/or SAFB granule formation reduces thermal resistance, indicating that these inhibitors are potential novel thermal sensitizers. However, SB366791 has limited proapop-

Received: November 17, 2025
Revised: February 2, 2026
Accepted: February 13, 2026
Published: February 18, 2026





https://doi.org/10.1021/acs.jmedchem.5c03361
J. Med. Chem. 2026, 69, 5944−5955

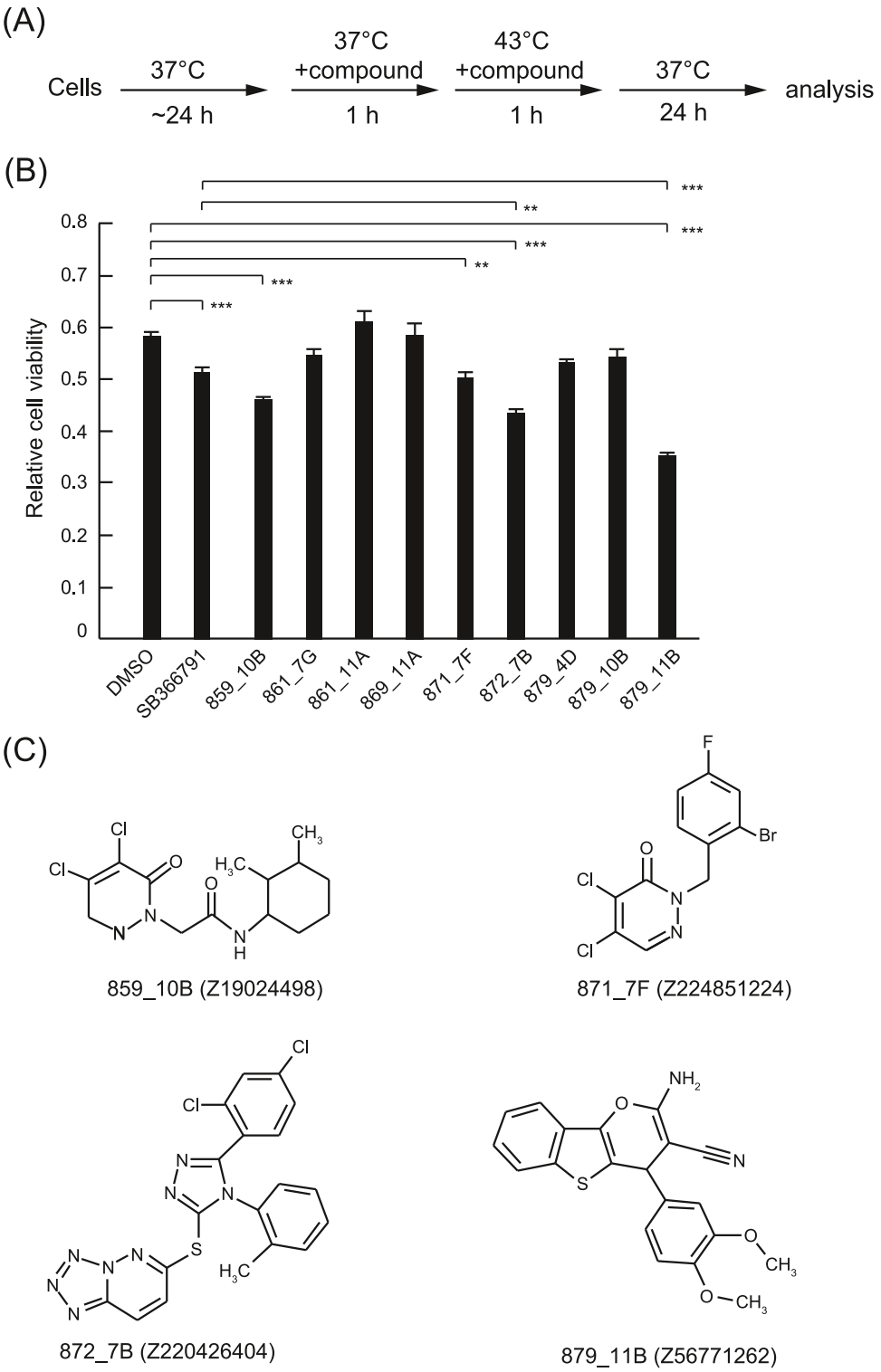


**Figure 1.** Compounds enhanced heat stress-induced cell growth inhibition in HeLa cells. (A) Schematic representation of cell treatment with the compounds. (B) Relative cell viability of cells treated with 5 $\mu$M compounds under heat stress. The viability of cells treated with dimethyl sulfoxide (DMSO) at 37 °C is defined as 1.0. Data are presented as the mean ± standard error of five independent experiments. *$P$ < 0.05, **$P$ < 0.01, and ***$P$ < 0.001; $P$-values are calculated using one-way analysis of variance and Tukey's multiple comparisons test. DMSO was used as a negative control and SB366791 as a positive control. (C) Structures of 859_10B (Z19024498), 871_7F (Z224851224), 872_7B (Z220426404), and 879_11B (Z56771262).

totic efficacy.[16] Furthermore, the transient receptor potential cation channel subfamily V1 (TRPV1) antagonists, including SB366791, induce hyperthermia and disrupt thermoregulation, thereby complicating temperature control during hyperthermia therapy[22] and increasing the risk of burns due to attenuated nociception.[23] Moreover, the suppression of $Ca^{2+}$ influx by TRPV1 antagonists may alter thermal responses and lead to unanticipated side effects. In addition, 2.5% 2,5-HD affects



https://doi.org/10.1021/acs.jmedchem.5c03361
J. Med. Chem. 2026, 69, 5944−5955

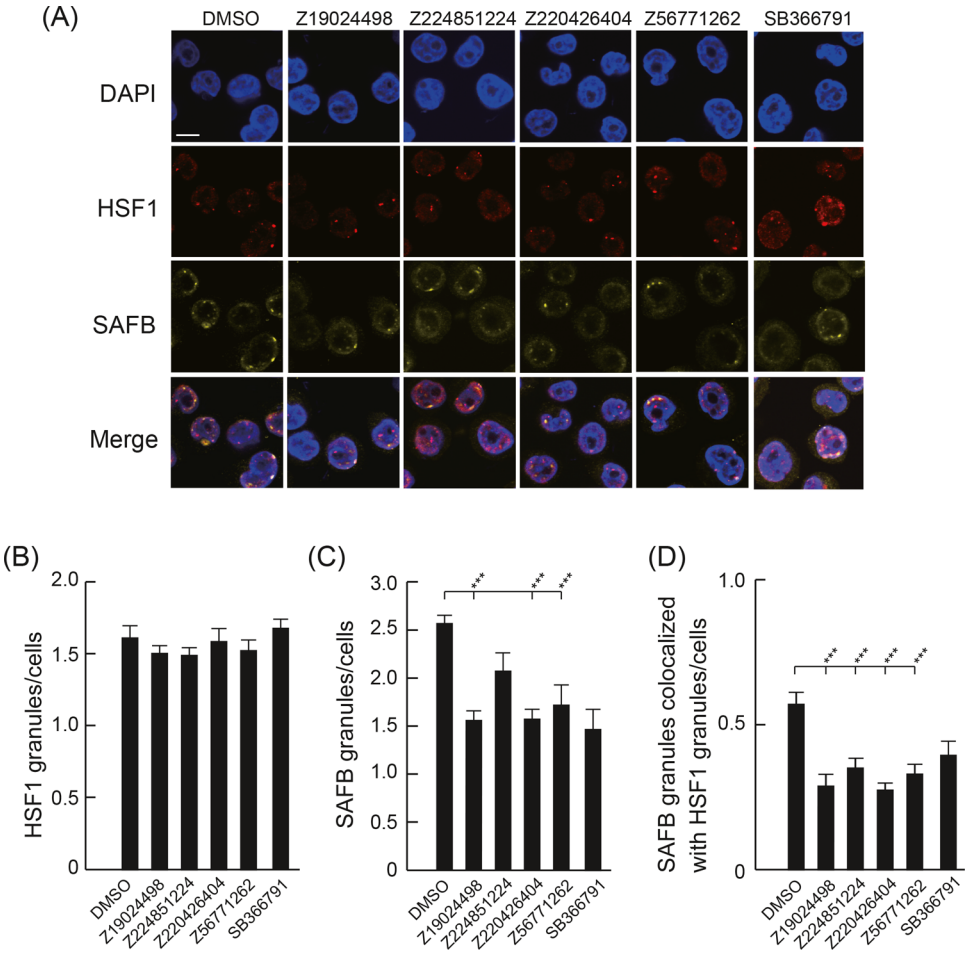


**Figure 2.** Inhibition of scaffold attachment factor B (SAFB) granule formation by compounds. (A) HeLa cells were exposed to heat stress at 43 °C for 1 h in the presence of 5 $\mu$M compound. Cells were stained with 4′,6-diamidino-2-phenylindole (blue), heat shock transcription factor 1 (HSF1) (red), and SAFB (yellow). Scale bars = 10 $\mu$m. The number of HSF1 (B) and SAFB (C) granules per cell are shown. (D) The number of SAFB granules colocalized with HSF1 granules per cell. Over 250 cells were counted. Data were presented as the mean ± standard error of seven independent experiments. *$P$ < 0.05, **$P$ < 0.01, and ***$P$ < 0.001; $P$-values were calculated using one-way analysis of variance and Dunnett's test by comparing dimethyl sulfoxide.

chromatin motion.[24] Additionally, although a Sat III RNA granule inhibitor (naphthyridine carbamate dimer) has been developed,[25] it remains unclear whether suppressing Sat III RNA granule formation enhances heat-induced apoptosis. Therefore, we screened a chemical compound library to identify novel compounds, functionally and structurally distinct from SB366791, that enhance heat-induced apoptosis by suppressing SAFB granule formation.

## RESULTS

### Identification of Compounds That Enhance Cell Growth Inhibition under Heat Stress

To identify novel hit compounds that enhance heat stress-induced apoptosis by inhibiting HSF1 and/or SAFB granules, we screened the Enamine PDR subset 2000 library of drug-like, representative diversity, and pharmacological diversity sets of 2000 compounds. However, an immunostaining-based assessment of their effects on HSF1 and SAFB granule formation may be time-consuming. SB366791 and 2,5-HD, which inhibit SAFB granule formation under heat stress, enhance heat stress-induced cell growth inhibition and apoptosis.[16] We hypothesized that compounds that enhance heat-induced cell growth inhibition act by inhibiting HSF1 or SAFB granule formation. Therefore, we analyzed cell viability under heat stress in the presence of compounds from the Enamine PDR subset 2000 using the Cell Counting Kit-8 (Figure 1A). SB366791 was used as a positive control. Based on this screening, we identified nine compounds that significantly enhanced heat stress-induced cell growth inhibition ($P$ < 0.01; Table S1).

To confirm reproducibility, we reanalyzed the nine compounds. As illustrated in Figure 1B,C, four compounds—859_10B (2-(4,5-dichloro-6-oxopyridazin-1-yl)-*N*-(2,3-dimethylcyclohexyl)acetamide, Z19024498), 871_7F (2-(2-bromo-4-fluorobenzyl)-4,5-dichloropyridazin-3(2h)-one, Z224851224), 872_7B (6-[[5-(2,4-dichlorophenyl)-4-(2-methylphenyl)-1,2,4-triazol-3-yl]sulfanyl]tetrazolo[1,5-*b*]-pyridazine, Z220426404), and 879_11B (2-amino-4-(3,4-dimethoxyphenyl)-4H-[1]benzothieno[3,2-*b*]pyran-3-carbonitrile, Z56771262)—enhanced heat stress-induced cell growth inhibition. Notably, under heat stress, cell growth in the presence of Z220426404 and Z56771262 was lower than that in the presence of SB366791. These results indicate that some of these compounds may inhibit heat stress-induced SAFB granule formation.


https://doi.org/10.1021/acs.jmedchem.5c03361
J. Med. Chem. 2026, 69, 5944−5955

### Inhibition of SAFB Granule Formation under Heat Stress in the Presence of Compounds

Using immunocytochemistry, we examined whether the four selected compounds inhibited SAFB granule formation under heat stress (Figure 2). Z19024498, Z220426404, and Z56771262 inhibited SAFB granule formation but did not affect HSF1 granule formation (Figure 2A−C). Additionally, these compounds inhibited SAFB granule formation, which colocalized with HSF1 granules (Figure 2A,D). These results indicate that the compounds inhibited both standalone SAFB granules and those that localized to nSBs.

Although Z224851224 did not inhibit the formation of HSF1 or SAF granules (Figure 2A−C), it inhibited the formation of SAFB granules that colocalized with HSF1 granules (Figure 2A,D). SAFB granules are localized to SLTM/Sam68 nuclear bodies (SNBs) under normal conditions,[26] and both SAFB and SLTM granules are localized into nSBs under heat stress.[27] Therefore, we examined the localization of SAFB and SLTM granules in the presence of Z224851224 under normal conditions. As shown in Figure S1, Z224851224 did not affect the formation of SAFB granules and SAFB granules colocalized with SLTM granules, although SLTM granule formation was slightly increased. These results suggest that the Z224851224-induced increase in SLTM granules formation under normal conditions may attenuate the compound's suppressive effect on SAFB granule formation.

### The Four Compounds Did Not Affect Heat Stress-Induced Increase in Intracellular $Ca^{2+}$ Levels and Sat III RNA Expression

The mechanism by which these compounds inhibit SAFB granule formation remains unclear. HSF1 is crucial for nSBs formation.[28] However, none of the four compounds affected HSF1 granule formation (Figure 2A,B).

The compounds may inhibit SAFB granule formation via a reduction in the SAFB expression levels. To test this hypothesis, we first examined whether compound treatment affected SAFB expression under normal or heat stress conditions using Western blot analysis (Figure S2). Under normal conditions, the expression levels of SAFB in cells treated with four compounds were comparable to those in DMSO-treated cells. Under heat stress, SAFB expression decreased in cells treated with DMSO, Z19024498, Z224851224, and Z220426404 and showed a slight decrease in Z56771262-treated cells. These results indicate that the inhibition of SAFB granule formation by the four compounds was independent of SAFB expression levels.

TRPV1 antagonist SB366791 inhibits heat stress-induced SAFB granule formation.[16] Additionally, SB366791 inhibited the heat stress-induced increase in intracellular $Ca^{2+}$ levels,[29] indicating that SAFB granule formation is likely dependent on the heat stress-induced increase in intracellular $Ca^{2+}$ levels. Therefore, we measured intracellular $Ca^{2+}$ levels in the presence of these four compounds under normal and heat stress conditions. Compared with DMSO, Z220426404 and Z56771262 did not affect basal or heat-induced $Ca^{2+}$ levels (Figure S3). Although intracellular $Ca^{2+}$ levels in the presence of Z19024498 and Z224851224 were 2-fold higher than those in DMSO, the ratio of the increase in intracellular $Ca^{2+}$ levels from 37 to 43 °C was similar among all four compounds and DMSO (Figure S3C). This indicates that the inhibition of SAFB granule formation by the four compounds occurs through a different pathway because it does not affect intracellular $Ca^{2+}$ levels.

The formation of SAFB granules was inhibited in Sat III RNA knockdown cells.[27] Therefore, we examined whether these four compounds inhibited the heat stress-induced increase in Sat III RNA expression. As illustrated in Figure S4, the Sat III RNA expression levels in the presence of compounds were similar to those in DMSO. This indicates that the inhibition of SAFB granule formation by the four compounds occurs through a different pathway because it does not affect the expression levels of Sat III RNA.

As shown in Figures S2−S4, SAFB protein levels, Sat III RNA expression, and intracellular $Ca^{2+}$ levels in the presence of the four hit compounds were comparable to those in the DMSO control, suggesting that these compounds suppress SAFB granule formation through a mechanism distinct from those of SB366791 and 2,5-HD.

### Determination of Half-Maximal Inhibitory Concentration ($IC_{50}$) Values for Standalone SAFB Granules and in Colocalization with HSF1 Granules

To determine the $IC_{50}$ values of the four compounds for (i) standalone SAFB granules, (ii) SAFB granules colocalized with HSF1 granules, and (iii) standalone HSF1 granules, the number of granules was plotted under various concentrations of each compound (Figures S5, S6, and S7). Z56771262 and Z224851224 exhibited the lowest $IC_{50}$ values for standalone SAFB granules and SAFB granules colocalized with HSF1 granules, respectively (Table 1). The $IC_{50}$ value of Z56771262 for SAFB granules colocalized with HSF1 granules was similar to that of Z19024498. Z220426404 exhibited the highest $IC_{50}$ values for standalone SAFB granules and SAFB granules colocalized with HSF1 granules. The $IC_{50}$ values of these compounds against standalone HSF1 granules were not determined because the HSF1 granules exhibited minimal suppression at various concentrations of each compound (Figure S7).

**Table 1. Half-Maximal Inhibitory Concentration Values for Compounds against Standalone Scaffold Attachment Factor B (SAFB) Granules and SAFB Granules Colocalized with Heat Shock Transcription Factor 1 Granules**

| | $IC_{50}$ ($\mu$M) | |
|---|---|---|
| compound | SAFB granules | SAFB granules colocalized with HSF1 |
| Z19024498 | 10.7 | 2.7 |
| Z224851224 | 29.6 | 1.9 |
| Z220426404 | 24.5 | 13.2 |
| Z56771262 | 6.2 | 2.9 |

### Determination of Half-Maximal Growth Inhibitory Concentration ($GI_{50}$) Values and the Thermal Enhancement Ratio (TER) for the Four Compounds

To determine the $GI_{50}$ values under normal and heat stress conditions, we analyzed cell viability at various compound concentrations in the HeLa, H1299, AsPC1, HepG2, and HEK293T cell lines (Table 2 and Figures S8, S9). Under heat stress, Z19024498 consistently exhibited $GI_{50}$ values lower than those under normal conditions across all five cell lines. The synergistic effect of heat and compound treatment was quantified using TER, which compares cell viability under normal and heat stress conditions (Table 2). All TER values for Z19024498 were >1.0, indicating that Z19024498 enhanced the hyperthermic effect in all cell lines.



https://doi.org/10.1021/acs.jmedchem.5c03361
J. Med. Chem. 2026, 69, 5944−5955

Table 2. Half-Maximal Growth Inhibitory Concentration and Thermal Enhancement Ratio Values for Compounds under Normal or Heat Stress Conditions[a]

| | | HeLa | | H1299 | | AsPC1 | | HepG2 | | HEK293T | |
|---|---|---|---|---|---|---|---|---|---|---|---|
| | | $GI_{50}$ ($\mu$M) | TER | $GI_{50}$ ($\mu$M) | TER | $GI_{50}$ ($\mu$M) | TER | $GI_{50}$ ($\mu$M) | TER | $GI_{50}$ ($\mu$M) | TER |
| Z19024498 | 37 °C | 5.3 | | 4.1 | | 18.7 | | 40.8 | | 10.5 | |
| | 43 °C | 3.1 | 1.7 | 1.6 | 2.6 | 15.6 | 1.2 | 3.4 | 12 | 6.0 | 1.8 |
| Z224851224 | 37 °C | 5.1 | | 3.3 | | N. D. | | N. D. | | 7.7 | |
| | 43 °C | 3.3 | 1.5 | 1.8 | 1.8 | N. D. | N. D. | 14.8 | N. D. | 4.8 | 1.6 |
| Z220426404 | 37 °C | 18.2 | | 9.8 | | N. D. | | 35.8 | | 21.0 | |
| | 43 °C | 3.6 | 5.1 | 2.0 | 4.9 | N. D. | N. D. | 7.6 | 4.7 | 6.1 | 3.4 |
| Z56771262 | 37 °C | 0.14 | | 0.25 | | 1.8 | | N. D. | | N. D. | |
| | 43 °C | 0.05 | 2.8 | 0.32 | 0.8 | 1.3 | 1.5 | <0.01 | N. D. | 10.1 | N. D. |

[a]N. D.: Not determined.

Additionally, Z224851224 and Z220426404 exhibited lower $GI_{50}$ values under heat stress than under normal conditions in all cell lines except AsPC1. Consistently, TER values for these compounds were >1.0 in the responsive cell lines. For Z56771262, the $GI_{50}$ values of cells treated under heat stress were lower than those treated under normal conditions without H1299 cells.

## Four Compounds Enhanced Heat Stress-Induced Apoptosis Efficiency

Our previous report demonstrated that SB366791 inhibited heat stress-induced SAFB granule formation and enhanced heat stress-induced apoptosis. To assess whether the four compounds similarly enhanced the efficiency of heat stress-induced apoptosis induction, apoptotic cells were detected using a NucView488 caspase-3 assay kit and PI, which can detect apoptotic and dead cells (Figure 3A). Z19024498, Z224851224, and Z220426404 enhanced heat stress-induced apoptosis efficiency in HeLa, H1299, AsPC1, HepG2, and HEK293T cell lines (Figure 3B−F). Additionally, the apoptosis-inducing efficacy of these compounds under heat stress was comparable to or greater than that of 5-FU and cisplatin, both of which are known thermal sensitizers.[5,6] Although Z56771262 induced stronger apoptosis under heat stress than did 5-FU and cisplatin in all cell lines, it did not enhance apoptosis in HeLa and H1299 cells.

## Z56771262 Induced Cell Cycle Arrest

All four compounds inhibited cell growth under normal conditions (Figures S8 and S9). However, their efficiency to induce apoptosis was relatively low (Figure 3). Chemotherapeutic drugs, such as cisplatin, are known to induce cell cycle arrest.[30] Therefore, we assessed whether these compounds induced cell cycle arrest (Figure 4). Z19024498, Z224851224, and Z220426404 did not significantly affect the cell cycle progression. In contrast, Z56771262 induced G2/M phase arrest, indicating that its inhibitory effect on cell growth was mediated through cell cycle arrest in the G2/M phase. However, the mechanisms underlying the growth inhibition by Z19024498, Z224851224, and Z220426404 remain unclear.

## A Combination of Z19024498 and Hyperthermia Effectively Suppressed Tumor Growth

In HeLa and H1299 cells, Z56771262 induced apoptosis more efficiently than Z19024498 in HeLa and H1299 cells at 43 °C; however, its apoptotic efficiency at 43 °C was comparable to that at 37 °C. Furthermore, Z56771262 induced cell death in HEK293 cells, suggesting the potential for unexpected side effects *in vivo*. Moreover, Z220426404 showed lower apoptotic efficiency than Z19024498 in HeLa and H1299 cells at 43 °C. Additionally, both the $IC_{50}$ value of Z220426404 for SAFB granules colocalized with HSF1 granules and its $GI_{50}$ value tended to be higher than those of Z19024498. Based on these observations, Z19024498 was selected for the *vivo* study.

To assess the effects of combining Z19024498 with hyperthermia, we used a human xenograft mouse model with HeLa cells. Once the tumor volume reached approximately 50−150 $mm^3$, the mice were intraperitoneally injected with either DMSO or Z19024498. One hour postinjection, the xenograft tumors were exposed to hyperthermia at 42.5 ± 0.3 °C for 10 min on days 0 and 8 (Figures 5A and S10A). Tumor growth was slightly inhibited in mice treated with Z19024498 than in those treated with DMSO (Figures 5A and S10B). Additionally, these mice exhibited a slightly longer lifespan in comparison to the DMSO-treated controls (Figure 5D).

Statistical analyses showed that the tumor volumes of xenografts treated with hyperthermia alone or in combination with Z19024498 were significantly reduced compared with those injected with DMSO or Z19024498 alone on day 14 (Figure 5A). However, by day 28, this difference became less significant owing to tumor regrowth in certain mice treated with the combination therapy that began at around day 22 (Figure S10B). As anticipated, tumor weight on day 28 was lower in the combination group than in the hyperthermia-only group (Figure 5C). Tumor regrowth following hyperthermia alone or in combination with thermal sensitizers such as 5-FU[31] or pifithrin-$\mu$[11] has been previously reported; therefore, the present results likely reflect a similar phenomenon.

Linear mixed-effect models were subsequently applied to assess differences in tumor growth over time (Figure 5B). Tumor volume in mice treated with Z19024498 alone was smaller than that in DMSO-treated mice, and hyperthermia treatment further reduced the tumor volume compared with Z19024498 alone. Notably, the combination of Z19024498 and hyperthermia significantly suppressed tumor growth compared with DMSO, Z19024498 alone, or hyperthermia alone.

Mice treated with both Z19024498 and hyperthermia exhibited a slightly extended lifespan compared with those treated with hyperthermia alone (Figure 5D). The body weights of mice in all treatment groups (DMSO, Z19024498, hyperthermia, and their combination) remained unaltered, indicating minimal to no physiological toxicity (Figure 5E).

## Target Protein Prediction of Hit Compounds

The target proteins of hit compounds Z19024498, Z224851224, Z220426404, and Z56771262 have not been determined. Therefore, we attempted to predict their potential target



https://doi.org/10.1021/acs.jmedchem.5c03361
J. Med. Chem. 2026, 69, 5944−5955

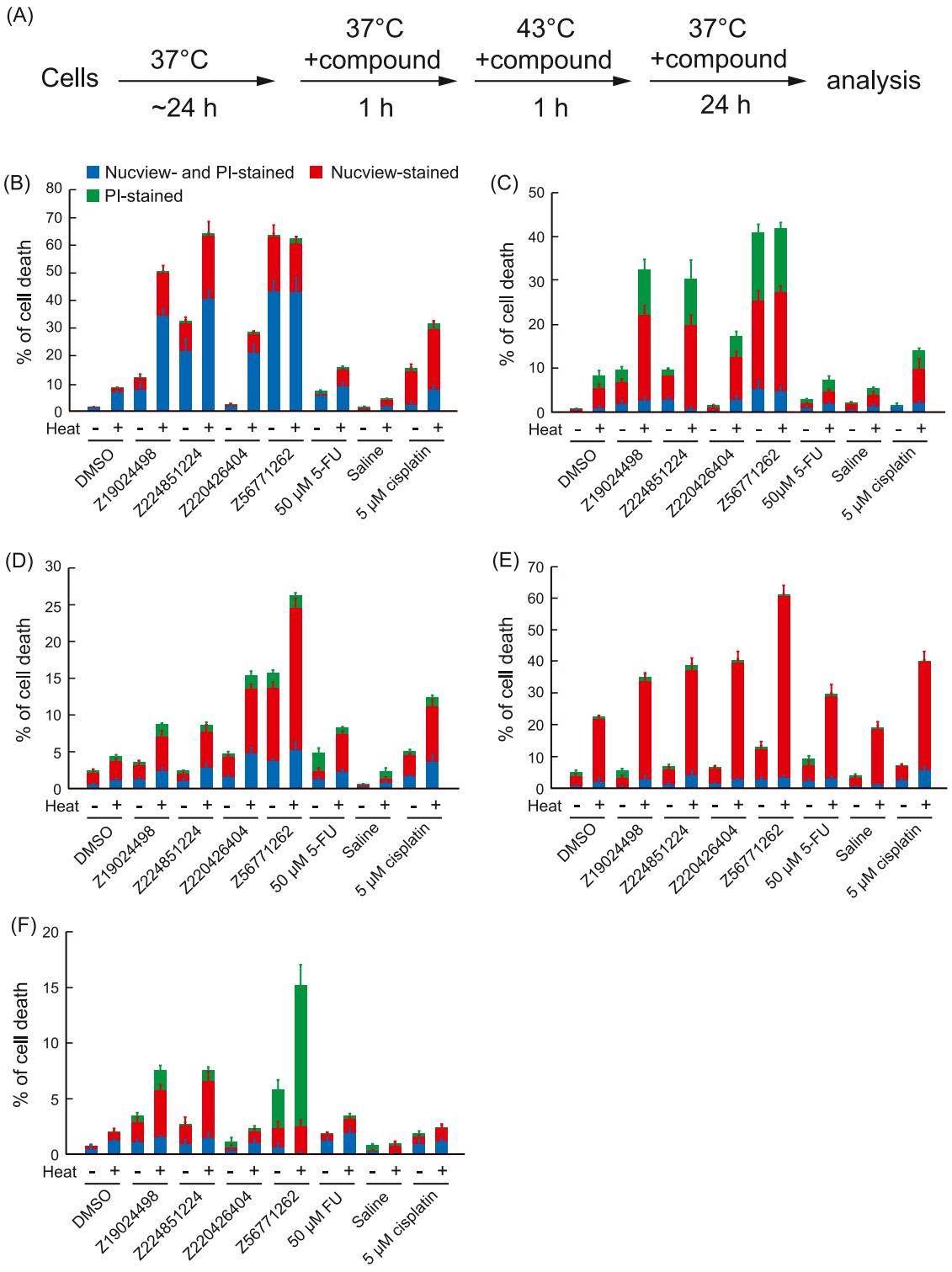


**Figure 3.** Apoptosis induction efficiency in the presence of compounds. (A) Schematic representation of cell treatment with the compounds used to detect the apoptosis induction efficiency. Apoptosis efficiencies were detected using NucView488 (green) and propidium iodide (PI) (red) in HeLa (B), H1299 (C), AsPC1 (D), HepG2 (E), and HEK293T (F) cell lines treated with 5 $\mu$M compounds or 50 $\mu$M 5-fluorouracil (5-FU) at 37 or 43 °C. Nonapoptotic cell death was detected using PI. Blue bars, NucView- and PI-stained cells; red bars, NucView-stained cells; and green bars, PI-stained cells. Data were presented as the mean ± standard error of six independent experiments. Over 200 cells were counted in each experiment. Cisplatin (5 $\mu$M) and 5-FU (50 $\mu$M) were used as positive controls.

proteins using several target prediction databases: Polypharmacology Browser 3,[32] TargetNet,[33] SwissTargetPrediction,[34] Similar Ensemble Approach,[35] and PharmMapper.[36] Proteins identified by at least two independent databases were selected. We then searched the public database to determine whether these candidate proteins have been reported to be involved in cell cycle regulation, cell growth, or apoptosis induction. As a result, no high-confidence target candidates were obtained for Z19024498 or Z56771262. In contrast, microphthalmia-associated transcription factor was predicted as a target of


https://doi.org/10.1021/acs.jmedchem.5c03361
J. Med. Chem. 2026, 69, 5944−5955

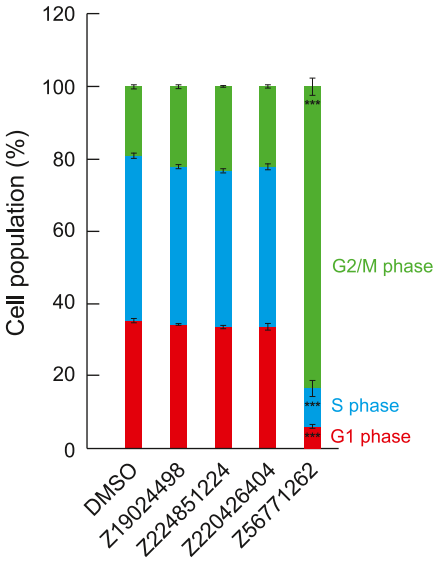


**Figure 4.** Effect of compounds on the cell cycle of HeLa cells. HeLa cells were treated with 5 $\mu$M compounds at 37 °C for 18 h. The cell cycle was analyzed using flow cytometry. Red bars, G1 phase; blue bars, S phase; and green bars, G2/M phase. Data were presented as the mean ± standard error of six independent experiments. Over 10,000 cells were counted in each experiment. *$P$ < 0.05, **$P$ < 0.01, and ***$P$ < 0.001; $P$-values were calculated using one-way analysis of variance and Dunnett's test by comparing dimethyl sulfoxide.

Z224851224, and the vascular endothelial growth factor receptor was predicted as a target of Z220426404. However, although these predicted proteins have been reported to be involved in the induction of cell death under oxidative stress, it remains unclear whether they also contribute to cell death induced by heat stress. Therefore, further investigation is warranted.

## DISCUSSION AND CONCLUSIONS

In this study, we identified novel compounds Z19024498, Z224851224, Z220426404, and Z56771262, that inhibit the formation of both standalone SAFB granules and SAFB granules colocalized with HSF1 granules. Additionally, these compounds enhanced the efficiency of heat stress-induced apoptosis. Moreover, the tumor volume of mice treated with the combination of Z19024498 and hyperthermia was significantly suppressed compared to that of mice treated with Z19024498 alone or hyperthermia alone on day 20 (Figure 5A). Therefore, these compounds, specifically, Z19022498, serve as potential sensitizers for applications in hyperthermia therapy. However, the tumor volume in mice treated with hyperthermia and Z19024498 increased in certain xenografts after day 22. The effect of hyperthermia itself showed a certain degree of variability (Figure S10B). In addition, since Z19024498 had a low solubility in PBS, it was administered with methyl cellulose. Therefore, the accumulation efficiency of Z19024498 in tumors may have varied, which could have resulted in the observed variability in the antitumor efficacy. To overcome these issues, it is necessary to determine the optimal conditions, including the concentration of Z19024498. Furthermore, the targeted delivery of Z19024498 using a drug delivery system may be required to achieve high local concentrations in the tumors. Additionally, because hyperthermia treatment for cancer is typically administered multiple times to manage thermal tolerance in cancer cells,[37] combining it repeatedly with Z19024498 may further enhance the antitumor effect.

We screened for hit compounds based on our hypothesis that compounds enhancing heat-induced cell growth inhibition act by inhibiting HSF1 and/or SAFB granule formation, resulting in the identification of four hit compounds. However, because no HSF1 granule formation inhibitors were identified, HSF1 or SAFB granule formation inhibitors that fall outside this hypothesis may also exist. Therefore, further analysis of the remaining nonhit compounds will be important in future studies.

Drug sensitivities and TER values of four compounds varied depending on the cell types (Tables 1 and 2, Figures 3 and 4). Genomic analysis of drug sensitivity in cancer databases indicates that sensitivity to anticancer agents tends to be highest in HeLa cells, followed by H1299 and AsPC1 cells.[38] Furthermore, drug sensitivity is influenced by the expression levels of ATP-binding cassette (ABC) transporters, such as ABCB1.[39] The Human Protein Atlas database (https://www.proteinatlas.org/) shows that ABCB1 expression is lower in HeLa cells than in AsPC1 cells. Therefore, the cell-type-dependent drug sensitivity and TER value observed for these compounds may be attributed, at least in part, to differences in ABC transporter expression.

The apoptosis-inducing efficiency of Z19024498 was equal to or higher than that of cisplatin and varied based on the cell type. This cell-type dependence limits its broad applicability across various cancers. In the future, structural optimization of Z19024498 can result in the development of lead compounds with apoptosis-inducing activity superior to that of cisplatin, independent of the cell type.

Z56771262 induced G2/M phase arrest and cell growth inhibition. In contrast, although Z19024498, Z224851224, and Z220426404 did not induce apoptosis or cell cycle arrest under normal conditions, they inhibited cell proliferation (Table 2 and Figures 3, 4). These results indicate that these compounds may prolong the cell doubling time. The doubling time of cells is closely associated with cell cycle progression and increase in the cell size.[40] Additionally, translational activity is associated with cell cycle progression and an increase in the cell size. For example, knockdown of the 60S ribosomal protein RPL11, which suppresses translation, does not affect cell cycle distribution or induce apoptosis but prolongs the doubling time.[41] This delay has been attributed to the delayed accumulation of cyclins A and E. Additionally, rapamycin, which inhibits the mammalian target of rapamycin complex 1 (mTORC1) that regulates the translational activity and cell size,[40] reduces the expression of cyclins A and E.[42] Therefore, Z19024498, Z224851224, and Z220426404 may prolong the cell doubling time by inhibiting translational regulators involved in translation-controlling signaling pathways such as phosphoinositide 3-kinase/protein kinase B (Akt)/mTOR.

Z56771262 efficiently induced apoptosis in cancer cell lines (Figure 3B–E), suggesting that it may serve as a potential anticancer agent. In addition, in HEK293T cells (non-cancerous), Z56771262 also induced apoptosis compared to the other three hit compounds (Figure 3F), indicating the potential for unexpected side effects. A previous report has shown that prolonged G2/M phase arrest promotes apoptosis induction.[43] Whereas the three compounds did not affect the cell cycle, Z56771262 induced G2/M phase arrest (Figure 4). Therefore, Z56771262 may induce apoptosis more efficiently in HEK293T cells than the three compounds.


https://doi.org/10.1021/acs.jmedchem.5c03361
J. Med. Chem. 2026, 69, 5944−5955

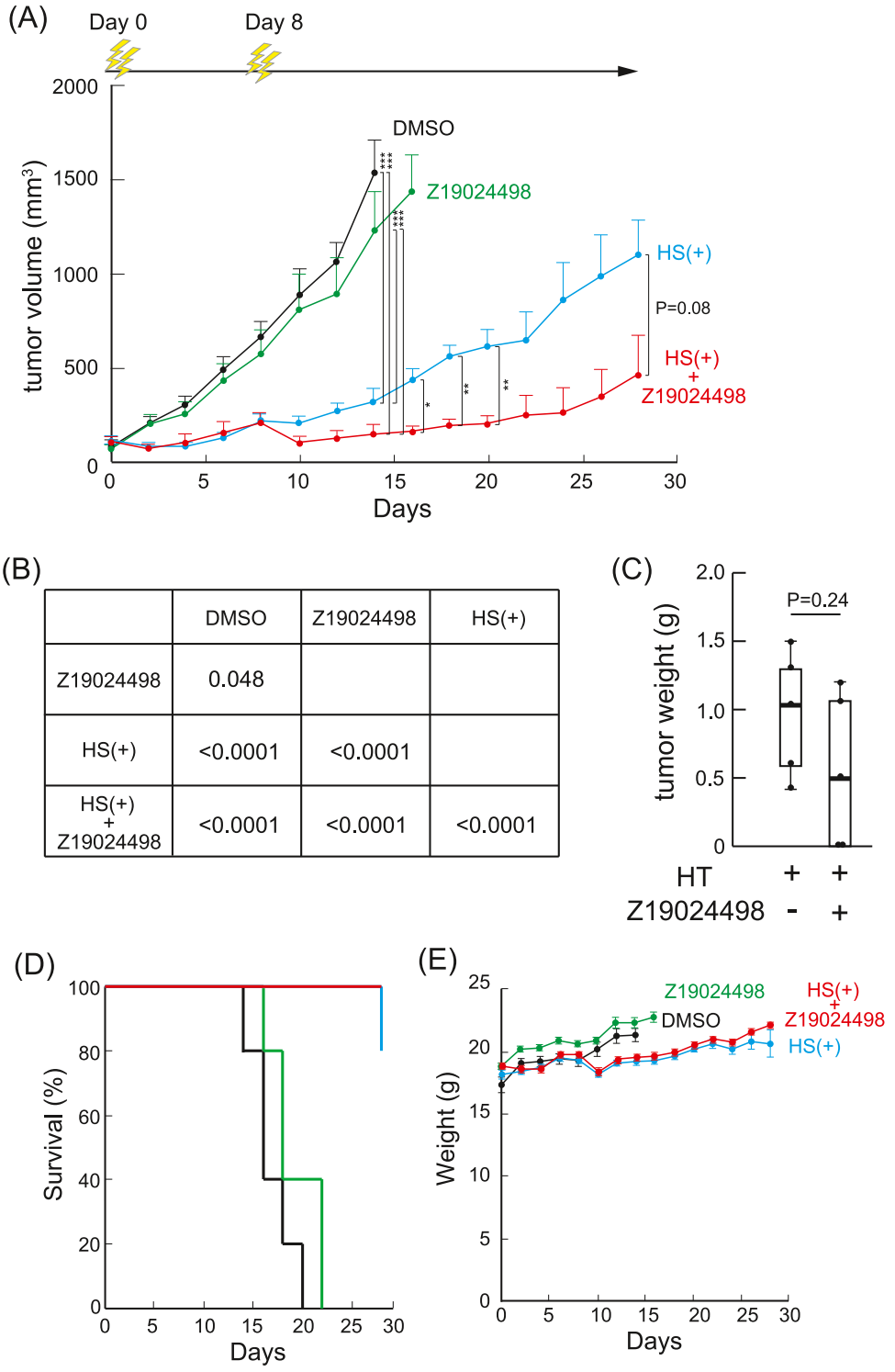


| | DMSO | Z19024498 | HS(+) |
|---|---|---|---|
| Z19024498 | 0.048 | | |
| HS(+) | <0.0001 | <0.0001 | |
| HS(+) + Z19024498 | <0.0001 | <0.0001 | <0.0001 |

**Figure 5.** Effect of the combination of Z19024498 and hyperthermia on tumor growth *in vivo*. (A) Schematic representation of cell treatment with compounds *in vivo* (upper panel). Time course of tumor volume in mice treated with dimethyl sulfoxide (HS-; black line), Z19024498 (green line), hyperthermia (HS+; blue line), and hyperthermia and Z19024498 (red line) (lower panel). Data were presented as the mean ± standard error ($n = 5$). $^{*}P < 0.05$, $^{**}P < 0.01$, and $^{***}P < 0.001$; *P*-values were calculated using Tukey's multiple comparison test for all groups on day 14 and Student's *t* test for comparisons between hyperthermia alone and the combination of Z19024498 and hyperthermia on days 16−28. (B) The *P*-values were determined using linear mixed-effects models. (C) Tumor weights of xenografts treated with hyperthermia or a combination of Z19024498 and hyperthermia on day 28. $^{*}P < 0.05$; *P*-values were calculated using Student's *t* test by comparing hyperthermia with the combination of Z19024498 and hyperthermia. (D) Survival curves of the xenografts after treatment for 28 days. (E) Mice body weights after different treatments.

The suppression of SAFB granules by Z19024498, Z224851224, Z220426404, and Z56771262 enhanced the efficiency of heat stress-induced apoptosis; however, the underlying mechanism remains unclear. Since SAFB regulates mRNA splicing,[44] SAFB granule formation may similarly modulate mRNA splicing under heat stress, thereby influencing


https://doi.org/10.1021/acs.jmedchem.5c03361
J. Med. Chem. 2026, 69, 5944−5955

the efficiency of apoptosis. Future studies examining mRNA splicing regulation in the presence of these compounds may provide important insights into the mechanism of apoptosis regulation mediated by the SAFB granule dynamics.

Although Z19024498, Z224851224, Z220426404, and Z56771262 inhibited the formation of both standalone SAFB granules and SAFB granules colocalized with HSF1 granules, the mechanism underlying this inhibition remains unclear. To understand the inhibition mechanism of these compounds, further assessment of their targets, including the predicted target proteins, is required. Furthermore, clarifying how these hit compounds inhibit SAFB granule formation will provide insight into the fundamental mechanisms underlying this process. These insights are anticipated to facilitate the development of more effective lead compounds. In addition, future studies, including clinical investigations, lead compound development, and validation of therapeutic efficacy will need to compare the effects of the hit and lead compounds with those of established heat sensitizers such as cisplatin and 5-FU.

## EXPERIMENTAL SECTION

### Cell Culture

HeLa cells (human carcinoma of the cervix) were cultured in Roswell Park Memorial Institute (RPMI) 1640 medium (Nacalai Tesque, Kyoto, Japan) containing 10% heat-inactivated fetal bovine serum (FBS) (Sigma-Aldrich, St. Louis, MO) and 1% antibiotic−antimycotic solution (Gibco, Gaithersburg, MD) at 37 °C in an atmosphere of 5% $CO_2$.

HepG2 cells (human liver cancer) were cultured in Dulbecco's modified Eagle's medium (low glucose) (Nacalai Tesque, Kyoto, Japan) containing 10% heat-inactivated FBS, 100 U/mL penicillin, and 100 μg/mL streptomycin (Gibco) in collagen-coated dishes at 37 °C in an atmosphere of 5% $CO_2$.

H1299 cells (p53-deficient human lung cancer) were cultured in RPMI 1640 medium (Nacalai Tesque, Kyoto, Japan) containing 10% heat-inactivated FBS and 1% antibiotic−antimycotic solution at 37 °C in an atmosphere of 5% $CO_2$.

AsPC1 cells (human pancreatic adenocarcinoma) were cultured in Dulbecco's modified Eagle's medium (high glucose) (Nacalai Tesque, Kyoto, Japan) containing 10% heat-inactivated FBS, 100 U/mL penicillin, and 100 μg/mL streptomycin at 37 °C in an atmosphere of 5% $CO_2$.

HEK293T cells (human embryonic kidney) were cultured in Dulbecco's modified Eagle's medium (high glucose) (Nacalai Tesque, Kyoto, Japan) containing 10% heat-inactivated FBS and 100 U/mL penicillin and 100 μg/mL streptomycin at 37 °C in an atmosphere of 5% $CO_2$.

The medium supplemented with either 10% FBS and 1% antibiotic−antimycotic solution or 100 U/mL penicillin and 100 μg/mL streptomycin—used to culture each cell line—is hereafter referred to as the growth medium.

### Screening of the Enamine PDR Subset 2000 Chemical Library

A library of 2000 compounds (Enamine PDR subset 2000; Enamine, Kyiv, Ukraine) was obtained from the Center for Supporting Drug Discovery and Life Science Research, Graduate School of Pharmaceutical Science, Osaka University. The compounds were stored in 1 mM stock solutions in dimethyl sulfoxide (DMSO). HeLa cells were seeded in 96-well plates the previous day (Figure 1A). The cells were treated with 5 μM compound in the growth medium at 37 °C for 1 h and incubated at 43 °C for 1 h. After exposure to heat stress, the cells were cultured in fresh growth medium at 37 °C for 24 h. Cell viability was measured using a Cell Counting Kit-8 (Dojindo, Kumamoto, Japan), following the manufacturer's protocol. A 15 μM SB366791 (Fujifilm Wako) was used as a positive control.[16]

### Immunocytochemistry

HeLa cells were seeded onto an 18-well μ-slide ibiTreat plate (ibidi, Munich, Germany) the previous day. The cells were treated with 0−20 μM of the following compounds—2-(4,5-dichloro-6-oxopyridazin-1-yl)-*N*-(2,3-dimethylcyclohexyl)acetamide (supplier's product code: Z19024498), 2-(2-bromo-4-fluorobenzyl)-4,5-dichloropyridazin-3(2h)-one (supplier's product code: Z224851224), 6-[[5-(2,4-dichlorophenyl)-4-(2-methylphenyl)-1,2,4-triazol-3-yl]sulfanyl]-tetrazolo[1,5-*b*]pyridazine (supplier's product code: Z220426404), and 2-amino-4-(3,4-dimethoxyphenyl)-4H-[1]benzothieno[3,2-*b*]-pyran-3-carbonitrile (supplier's product code: Z56771262) (Enamine) in a growth medium at 37 °C for 1 h, followed by incubation at 43 °C for 1 h. The purities of all compounds were greater than 95%. Immunocytochemistry was performed as described previously.[16] The primary antibodies used were rabbit anti-HSF1 (1:1000; Cell Signaling Technology, Danvers, MA), mouse anti-SAF-B (1:200; Abnova, Taipei, Taiwan), and rabbit anti-SAFB-like transcription modulator (SLTM; 1:300; Sigma-Aldrich, St. Louis, MO). Alexa 546- and Alexa 647-conjugated secondary antibodies were purchased from Invitrogen, and 4′,6-diamidino-2-phenylindole (DAPI) was obtained from Dojindo (Kumamoto, Japan). The stained cells were examined with a confocal microscope (FV-1000; Olympus, Tokyo, Japan). HSF1 and SAFB granules larger than 0.5 $\mu m^2$ and exhibiting high fluorescence intensity were counted. A 15 μM SB366791 was used as a positive control.

### Half-Maximal Inhibitory Concentration ($IC_{50}$) Index Calculation

To calculate $IC_{50}$ values for SAFB granules colocalized with HSF1 granules, standalone SAFB granules, and standalone HSF1 granules, data from the immunochemistry assay in the presence of compounds in a concentration-dependent manner were analyzed using a four-parameter logistic (4PL) curve calculator (AAT Bioquest Web site [https://www.aatbio.com/tools/four-parameter-logistic-4pl-curve-regression-online-calculator]).

### Analysis of Sat III RNA Expression Level in the Presence of Compounds

HeLa cells were treated with 5 μM compound in the growth medium at 37 °C for 1 h and incubated at 43 °C for 1 h. After treatment, the cells were suspended in RNAiso Plus (TaKaRa, Otsu, Japan) for total RNA extraction following the manufacturer's protocol. To determine Sat III RNA expression levels, total RNA (500 ng) was subjected to a real-time polymerase chain reaction (PCR). The mRNA was reverse-transcribed into cDNA using a PrimeScript RT reagent kit with gDNA eraser (TaKaRa, Otsu, Japan). The RSM13 primer described by Valgardsdottir et al. was used to reverse-transcribe Sat III RNA.[45] qPCR was performed using KOD SYBR qPCR mix (TOYOBO, Osaka, Japan) on a detection system (CronoSTAR 96; Clontech, Otsu, Japan) with specific oligonucleotide primers: glyceraldehyde-3-phosphate dehydrogenase (GAPDH) (sense 5′-ATT CCA CCC ATG GCA AAT TC-3′ and antisense 5′-GGG ATT TCC ATT GAT GAC AAG C-3′) and Sat III RNA (sense 5′-CCG TAA ACG ACG GCC AG-3′ and antisense 5′-AAT CAA CCC GAG TGC AAT CG-3′). Sat III RNA expression was normalized to GAPDH expression levels using the $2^{-\Delta\Delta Ct}$ method.

### Observation of Intracellular $Ca^{2+}$ Levels in the Presence of Reagents Using Fluo4-AM

After HeLa cells were treated with 5 μM compounds in the growth medium at 37 °C for 30 min, 10 μM Fluo4-AM was added. The cells were incubated for an additional 30 min and then were exposed to heat stress at 43 °C for 30 min. Fluo4-AM fluorescence was observed using an IX51 fluorescence microscope (Olympus, Tokyo, Japan).

### Western Blot Analysis

The cells were treated with 5 μM compound in the growth medium at 37 °C for 1 h and incubated at 43 °C for 1 h. Total protein was extracted using RIPA buffer (50 mM Tris-HCl pH 7.6, 150 mM KCl, 1% NP-40, 1% sodium deoxycholate, 0.1% sodium dodecyl sulfate, and protease inhibitor cocktail (Wako Pure Chemical Industries)), and Western blot analysis was performed as described previously.[16] Rabbit anti-SAF-B (dilution 1:10000, Proteintech, Tokyo, Japan) and rabbit anti-α-


https://doi.org/10.1021/acs.jmedchem.5c03361
J. Med. Chem. 2026, 69, 5944−5955

tubulin (dilution 1:1000, Cell singling technology, Danvers, MA) were used. Band intensities were detected and quantified using an iBright1500 (ThermoFisher Scientific, Sunnyvale, CA).

### Detection of Apoptotic Cells Using NuView488 Caspase-3 Substrate and Propidium Iodide (PI)

Cells were treated with 5 $\mu$M compound in the growth medium at 37 °C for 1 h and incubated at 43 °C for 1 h. After exposure to heat stress, the cells were cultured in a growth medium containing 5 $\mu$M compound at 37 °C for 24 h (Figure 3A). Apoptosis was detected using the NucView488 caspase-3 substrate (Biotium, Fremont, CA) and PI (Molecular Probes, Eugene, OR). The apoptotic cells were visualized using an Olympus IX51 fluorescence microscope. As a positive control, 50 $\mu$M 5-FU (Wako Pure Chemical Industries) dissolved in DMSO and 5 $\mu$M cisplatin (Wako Pure Chemical Industries) dissolved in saline were used.

### Half-Maximal Growth Inhibitory Concentration ($GI_{50}$) and Thermal Enhancement Ratio Index Calculation

The cells were treated with 0−25 $\mu$M compound in the growth medium at 37 °C for 1 h, followed by incubation at 43 °C for 1 h. After exposure to heat stress, the cells were cultured in a growth medium containing 5 $\mu$M compound at 37 °C for 24 h. Cell viability was measured using Cell Counting Kit-8. The $GI_{50}$ values were calculated using a 4PL curve calculator (AAT BioQuest Web site).

The thermal enhancement ratio (TER) was calculated by dividing the compound dose required to inhibit cell viability by 50% without hyperthermia by the compound dose required to achieve the same effect with hyperthermia.

### Cell Cycle Analysis

HeLa cells were treated with 5 $\mu$M compound in the growth medium at 37 °C for 18 h. The cells were incubated in a growth medium supplemented with 5 $\mu$M bromodeoxyuridine (BrdU; Sigma-Aldrich) for 15 min in an atmosphere of 5% $CO_2$. After treatment, the cells were fixed with 70% ethanol at −30 °C overnight. The fixed cells were permeabilized in 2 M HCl containing 0.5% Triton X-100 for 30 min at room temperature. The cells were incubated with 0.1 M sodium tetraborate for 5 min at room temperature and then rinsed with Dulbecco's phosphate-buffered saline (D-PBS) containing 0.5% bovine serum albumin (BSA). The cells were incubated with rabbit anti-BrdU (1:400; Cell Signaling Technology, Danvers, MA) diluted in D-PBS containing 0.5% BSA for 1 h at room temperature. Unbound antibodies were removed by washing twice with D-PBS. Subsequently, the cells were incubated with Alexa 488-conjugated secondary antibodies (1:1000; Invitrogen, Carlsbad, CA) for 1 h at room temperature. Unbound antibodies were removed by washing twice with 1× D-PBS and incubated with Guava cell cycle reagent containing PI (Merck Millipore, Burlington, MA) for 30 min at room temperature. Fluorescence intensities were measured using a Guava easyCyte 6−2L flow cytometer (Merck Millipore).

### *In Vivo* Hyperthermia with a Potential Thermal Sensitizer

All animal experiments were approved by the Animal Care and Use Committee of Okayama University (OKU-2024581). Six-week-old female nude mice (BALB/c-nu/nu) (The Jackson Laboratory, Yokohama, Japan) were subcutaneously injected in the thigh with HeLa cells ($2.5 \times 10^6$ cells) suspended in 100 $\mu$L of D-PBS containing 30% Matrigel Matrix (Corning, Life Science, Bedford, MA).

Z19024498 was initially dissolved in DMSO, and 0.5 w/v% methyl cellulose 400 (Fujifilm Wako) was added to achieve a final DMSO concentration of 6%. After the tumor volume reached approximately 50−150 $mm^3$, the mice were randomly divided into four groups (five mice per group). Each mouse was intraperitoneally injected with 100 $\mu$L of 0.5% w/v methyl cellulose 400 containing 6% DMSO or Z19024498 (3 mg/kg). Hyperthermia treatment was performed using Thermotron-RF I.V. (Yamamoto Vinita Ltd., Osaka, Japan) at 42.5 ± 0.3 °C for 10 min (electrode size: 20 mm; maximum output: 100 W).

Body weight and tumor volume were monitored every 2 days for up to 28 days following hyperthermia. The tumor volume was measured using a caliper and calculated using the following formula: length × $width^2 \times 0.5$.[46] The tumor weight was measured in mice with tumor sizes exceeding 1900 $mm^3$ or in mice 28 days after treatment. Following the Animal Protection Law, the mice were euthanized when the tumor volume exceeded 1900 $mm^3$ or when their weight was significantly reduced.

### Statistical Analysis

All results are expressed as the mean ± standard error of the mean. R[47] and EZR[48] softwares were used for statistical analyses. The number of experimental replicates is demonstrated in the figure legends.

## ■ ASSOCIATED CONTENT

### Supporting Information

The Supporting Information is available free of charge at https://pubs.acs.org/doi/10.1021/acs.jmedchem.5c03361.

SAFB and SLTM granule formation, SAFB expression level, intracellular $Ca^{2+}$ concentration, satellite III expression, number of SAFB granules colocalized with HSF1 granules, number of SAFB granules, number of HSF1 granules, concentration-dependent inhibition of cell growth in HeLa, H1299, and AsPC1 cells, concentration-dependent inhibition of cell growth in HepG2 and HEK293 cells, suppression of tumor growth by combination of hyperthermia and Z19024498 (PDF)

Cell growth in the presence of compounds by screening (XLSX)

Molecular formula strings (CSV)

## ■ AUTHOR INFORMATION


### Corresponding Author

**Kazunori Watanabe** − *Faculty of Interdisciplinary Science and Engineering in Health Systems, Okayama University, Okayama 7008530, Japan;* orcid.org/0000-0003-3678-636X; Email: k_watanabe@okayama-u.ac.jp

### Authors

**Yuji Furutani** − *Faculty of Interdisciplinary Science and Engineering in Health Systems, Okayama University, Okayama 7008530, Japan*

**Natsuki Shimasaki** − *Faculty of Interdisciplinary Science and Engineering in Health Systems, Okayama University, Okayama 7008530, Japan*

**Riko Yamada** − *Faculty of Interdisciplinary Science and Engineering in Health Systems, Okayama University, Okayama 7008530, Japan*

**Takashi Ohtsuki** − *Faculty of Interdisciplinary Science and Engineering in Health Systems, Okayama University, Okayama 7008530, Japan;* orcid.org/0000-0002-3183-5305

Complete contact information is available at: https://pubs.acs.org/10.1021/acs.jmedchem.5c03361


### Author Contributions

Y.F., N.S. and R.Y.: formal analysis, writing—review and editing; T.O.: writing—review and editing; K.W.: data curation, formal analysis, investigation, visualization, conceptualization, funding acquisition, project administration, supervision, writing—original draft, writing—review and editing.

### Notes

The authors declare no competing financial interest.



https://doi.org/10.1021/acs.jmedchem.5c03361
J. Med. Chem. 2026, 69, 5944−5955

## ■ ACKNOWLEDGMENTS

This work was supported by the Wesco Scientific Promotion Foundation, a 2024 research grant from Amano Institute of Technology (to K.W.). This research was partially supported by Platform Project for Supporting Drug Discovery and Life Science Research (Basis for Supporting Innovative Drug Discovery and Life Science Research (BINDS)) from AMED under Grant Number JP21am0101084. We would like to thank Editage (www.editage.jp) for English language editing.

## ■ ABBREVIATIONS

2,5-HD, 2,5-hexanediol; 5-FU, 5-fluorouracil; Akt, phosphoinositide 3-kinase/protein kinase B; BrdU, bromodeoxyuridine; BSA, bovine serum albumin; DAPI, 4′,6-diamidino-2-phenylindole; D-PBS, Dulbecco's phosphate-buffered saline; FBS, fetal bovine serum; $GI_{50}$, half-maximal growth inhibitory concentration; HSF1, heat shock transcription factor 1; HSP, heat shock protein; HSP70, 70 kDa heat shock protein; HSP90, 90 kDa heat shock protein; nSBs, nuclear stress bodies; PI, propidium iodide; qPCR, quantitative polymerase chain reaction; SAFB, scaffold attachment factor B; Sat III RNA, satellite III long noncoding RNA; SGs, stress granules; SLTM, SAFB-like transcription modulator; SNBs, SLM/Sam68 nuclear bodies; TER, thermal enhancement ratio; TRPV1, transient receptor potential vanilloid 1

## ■ REFERENCES

(1) Chang, D.; Lim, M.; Goos, J. A. C. M.; Qiao, R.; Ng, Y. Y.; Mansfeld, F. M.; Jackson, M.; Davis, T. P.; Kavallaris, M. Biologically Targeted Magnetic Hyperthermia: Potential and Limitations. *Front. Pharmacol.* **2018**, *9*, No. 831.

(2) Palzer, R. J.; Heidelberger, C. Studies on the Quantitative Biology of Hyperthermic Killing of HeLa Cells. *Cancer Res.* **1973**, *33* (2), 415−421.

(3) Zhou, S.; Tsutsumiuchi, K.; Imai, R.; Miki, Y.; Kondo, A.; Nakagawa, H.; Watanabe, K.; Ohtsuki, T. In Vitro Study of Tumor-Homing Peptide-Modified Magnetic Nanoparticles for Magnetic Hyperthermia. *Molecules* **2024**, *29* (11), No. 2632.

(4) Samali, A.; Holmberg, C. I.; Sistonen, L.; Orrenius, S. Thermotolerance and Cell Death Are Distinct Cellular Responses to Stress: Dependence on Heat Shock Proteins. *FEBS Lett.* **1999**, *461* (3), 306−310.

(5) Zhang, X.; Liu, T.; Ye, Y.; Zhu, A.; Yang, Z.; Fu, Y.; Wei, C.; Liu, Q.; Zhao, C.; Wang, G. Hyperthermia Combined with 5-Fluorouracil Promoted Apoptosis and Enhanced Thermotolerance in Human Gastric Cancer Cell Line SGC-7901. *Onco. Targets Ther.* **2015**, 1265.

(6) Raaphorst, G. P.; Doja, S.; Davis, L.; Stewart, D.; Ng, C. E. A Comparison of Hyperthermia Cisplatin Sensitization in Human Ovarian Carcinoma and Glioma Cell Lines Sensitive and Resistant to Cisplatin Treatment. *Cancer Chemother. Pharmacol.* **1996**, *37* (6), 574−580.

(7) Cheng, Y.; Weng, S.; Yu, L.; Zhu, N.; Yang, M.; Yuan, Y. The Role of Hyperthermia in the Multidisciplinary Treatment of Malignant Tumors. *Integr. Cancer Ther.* **2019**, *18*, No. 1534735419876345.

(8) Vriend, L. E. M.; van den Tempel, N.; Oei, A. L.; L'Acosta, M.; Pieterson, F. J.; Franken, N. A. P.; Kanaar, R.; Krawczyk, P. M. Boosting the Effects of Hyperthermia-Based Anticancer Treatments by HSP90 Inhibition. *Oncotarget* **2017**, *8* (57), 97490−97503.

(9) Huang, Z.; Zhou, X.; He, Y.; Ke, X.; Wen, Y.; Zou, F.; Chen, X. Hyperthermia Enhances 17-DMAG Efficacy in Hepatocellular Carcinoma Cells with Aggravated DNA Damage and Impaired G2/M Transition. *Sci. Rep.* **2016**, *6* (1), No. 38072.

(10) Miyagawa, T.; Saito, H.; Minamiya, Y.; Mitobe, K.; Takashima, S.; Takahashi, N.; Ito, A.; Imai, K.; Motoyama, S.; Ogawa, J. Inhibition of Hsp90 and 70 Sensitizes Melanoma Cells to Hyperthermia Using Ferromagnetic Particles with a Low Curie Temperature. *Int. J. Clin. Oncol.* **2014**, *19* (4), 722−730.

(11) Sekihara, K.; Harashima, N.; Tongu, M.; Tamaki, Y.; Uchida, N.; Inomata, T.; Harada, M. Pifithrin-$\mu$, an Inhibitor of Heat-Shock Protein 70, Can Increase the Antitumor Effects of Hyperthermia Against Human Prostate Cancer Cells. *PLoS One* **2013**, *8* (11), No. e78772.

(12) Rastogi, S.; Joshi, A.; Sato, N.; Lee, S.; Lee, M.-J.; Trepel, J. B.; Neckers, L. An Update on the Status of HSP90 Inhibitors in Cancer Clinical Trials. *Cell Stress Chaperones* **2024**, *29* (4), 519−539.

(13) Biamonti, G.; Vourc'h, C. Nuclear Stress Bodies. *Cold Spring Harb. Perspect. Biol.* **2010**, *2* (6), No. a000695.

(14) Frydrýšková, K.; Mašek, T.; Pospíšek, M. Changing Faces of Stress: Impact of Heat and Arsenite Treatment on the Composition of Stress Granules. *WIREs RNA* **2020**, *11* (6), No. e1596.

(15) Hofmann, S.; Kedersha, N.; Anderson, P.; Ivanov, P. Molecular Mechanisms of Stress Granule Assembly and Disassembly. *Biochim. Biophys. Acta, Mol. Cell Res.* **2021**, *1868* (1), No. 118876.

(16) Watanabe, K.; Ohtsuki, T. Inhibition of Hsf1 and Safb Granule Formation Enhances Apoptosis Induced by Heat Stress. *Int. J. Mol. Sci.* **2021**, *22* (9), No. 4982.

(17) Ninomiya, K.; Adachi, S.; Natsume, T.; Iwakiri, J.; Terai, G.; Asai, K.; Hirose, T. LncRNA-dependent Nuclear Stress Bodies Promote Intron Retention through SR Protein Phosphorylation. *EMBO J.* **2020**, *39* (3), No. e102729.

(18) Cotto, J. J.; Fox, S. G.; Morimoto, R. I. HSF1 Granules: A Novel Stress-Induced Nuclear Compartment of Human Cells. *J. Cell Sci.* **1997**, *110* (23), 2925−2934.

(19) Weighardt, F.; Cobianchi, F.; Cartegni, L.; Chiodi, I.; Villa, A.; Riva, S.; Biamonti, G. A Novel HnRNP Protein (HAP/SAF-B) Enters a Subset of HnRNP Complexes and Relocates in Nuclear Granules in Response to Heat Shock. *J. Cell Sci.* **1999**, *112*, 1465−1476.

(20) Jolly, C.; Metz, A.; Govin, J.; Vigneron, M.; Turner, B. M.; Khochbin, S.; Vourc'h, C. Stress-Induced Transcription of Satellite III Repeats. *J. Cell Biol.* **2004**, *164* (1), 25−33.

(21) Miyagawa, R.; Mizuno, R.; Watanabe, K.; Ijiri, K. Formation of TRNA Granules in the Nucleus of Heat-Induced Human Cells. *Biochem. Biophys. Res. Commun.* **2012**, *418* (1), 149−155.

(22) Gavva, N. R.; Treanor, J. J. S.; Garami, A.; Fang, L.; Surapaneni, S.; Akrami, A.; Alvarez, F.; Bak, A.; Darling, M.; Gore, A.; Jang, G. R.; Kesslak, J. P.; Ni, L.; Norman, M. H.; Palluconi, G.; Rose, M. J.; Salfi, M.; Tan, E.; Romanovsky, A. A.; Banfield, C.; Davar, G. Pharmacological Blockade of the Vanilloid Receptor TRPV1 Elicits Marked Hyperthermia in Humans. *Pain* **2008**, *136* (1), 202−210.

(23) Moran, M. M.; Szallasi, A. Targeting Nociceptive **Transient Receptor Potential** Channels to Treat Chronic Pain: Current State of the Field. *Br. J. Pharmacol.* **2018**, *175* (12), 2185−2203.

(24) Itoh, Y.; Iida, S.; Tamura, S.; Nagashima, R.; Shiraki, K.; Goto, T.; Hibino, K.; Ide, S.; Maeshima, K. 1,6-Hexanediol Rapidly Immobilizes and Condenses Chromatin in Living Human Cells. *Life Sci. Alliance* **2021**, *4* (4), No. e202001005.

(25) Shibata, T.; Nagano, K.; Ueyama, M.; Ninomiya, K.; Hirose, T.; Nagai, Y.; Ishikawa, K.; Kawai, G.; Nakatani, K. Small Molecule Targeting r(UGGAA)n Disrupts RNA Foci and Alleviates Disease Phenotype in Drosophila Model. *Nat. Commun.* **2021**, *12* (1), No. 236.

(26) Rajan, P.; Dalgliesh, C.; Bourgeois, C. F.; Heiner, M.; Emami, K.; Clark, E. L.; Bindereif, A.; Stevenin, J.; Robson, C. N.; Leung, H. Y.; Elliott, D. J. Proteomic Identification of Heterogeneous Nuclear Ribonucleoprotein L as a Novel Component of SLM/Sam68 Nuclear Bodies. *BMC Cell Biol.* **2009**, *10*, 82.

(27) Aly, M. K.; Ninomiya, K.; Adachi, S.; Natsume, T.; Hirose, T. Two Distinct Nuclear Stress Bodies Containing Different Sets of RNA-Binding Proteins Are Formed with HSATIII Architectural Noncoding RNAs upon Thermal Stress Exposure. *Biochem. Biophys. Res. Commun.* **2019**, *516* (2), 419−423.

(28) Gavrilova, A. A.; Fefilova, A. S.; Vishnyakov, I. E.; Kuznetsova, I. M.; Turoverov, K. K.; Uversky, V. N.; Fonin, A. V. On the Roles of the Nuclear Non-Coding RNA-Dependent Membrane-Less Organelles in the Cellular Stress Response. *Int. J. Mol. Sci.* **2023**, *24* (9), No. 8108.



https://doi.org/10.1021/acs.jmedchem.5c03361
J. Med. Chem. 2026, 69, 5944−5955

(29) Obi, S.; Nakajima, T.; Hasegawa, T.; Kikuchi, H.; Oguri, G.; Takahashi, M.; Nakamura, F.; Yamasoba, T.; Sakuma, M.; Toyoda, S.; Tei, C.; Inoue, T. Heat Induces Interleukin-6 in Skeletal Muscle Cells via TRPV1/PKC/CREB Pathways. *J. Appl. Physiol.* **2017**, *122*, 683−694.
(30) Velma, V.; Dasari, S. R.; Tchounwou, P. B. Low Doses of Cisplatin Induce Gene Alterations, Cell Cycle Arrest, and Apoptosis in Human Promyelocytic Leukemia Cells. *Biomark. Insights* **2016**, *11*, 113−121.
(31) Tsumura, M.; Yoshiga, K.; Takada, K. Enhancement of Antitumor Effects of 1-Hexylcarbamoyl-5-Fluorouracil Combined with Hyperthermia on Ehrlich Ascites Tumor in Vivo and Nakahara-Fukuoka Sarcoma Cell in Vitro. *Cancer Res.* **1988**, *48* (14), 3977−3980.
(32) Darsaraee, M.; Javor, S.; Reymond, J.-L.Polypharmacology Browser PPB3: A Web-Based Deep Learning Tool for Target Prediction Using ChEMBL Data *ChemRxiv* 2025 DOI: 10.26434/chemrxiv-2025-rlgq5-v2.
(33) Yao, Z.-J.; Dong, J.; Che, Y.-J.; Zhu, M.-F.; Wen, M.; Wang, N.-N.; Wang, S.; Lu, A.-P.; Cao, D.-S. TargetNet: A Web Service for Predicting Potential Drug−Target Interaction Profiling via Multi-Target SAR Models. *J. Comput.-Aided. Mol. Des.* **2016**, *30* (5), 413−424.
(34) Daina, A.; Michielin, O.; Zoete, V. SwissTargetPrediction: Updated Data and New Features for Efficient Prediction of Protein Targets of Small Molecules. *Nucleic Acids Res.* **2019**, *47* (W1), W357−W364.
(35) Keiser, M. J.; Roth, B. L.; Armbruster, B. N.; Ernsberger, P.; Irwin, J. J.; Shoichet, B. K. Relating Protein Pharmacology by Ligand Chemistry. *Nat. Biotechnol.* **2007**, *25* (2), 197−206.
(36) Wang, X.; Shen, Y.; Wang, S.; Li, S.; Zhang, W.; Liu, X.; Lai, L.; Pei, J.; Li, H. PharmMapper 2017 Update: A Web Server for Potential Drug Target Identification with a Comprehensive Target Pharmacophore Database. *Nucleic Acids Res.* **2017**, *45* (W1), W356−W360.
(37) Fan, Y.-F.; Qin, Y.; Li, D.-G.; Kerr, D. Retrospective Clinical Study of Advanced Pancreatic Cancer Treated With Chemotherapy and Abdominal Hyperthermia. *J. Glob. Oncol.* **2018**, *2018* (4), 1−4.
(38) Yang, W.; Soares, J.; Greninger, P.; Edelman, E. J.; Lightfoot, H.; Forbes, S.; Bindal, N.; Beare, D.; Smith, J. A.; Thompson, I. R.; Ramaswamy, S.; Futreal, P. A.; Haber, D. A.; Stratton, M. R.; Benes, C.; McDermott, U.; Garnett, M. J. Genomics of Drug Sensitivity in Cancer (GDSC): A Resource for Therapeutic Biomarker Discovery in Cancer Cells. *Nucleic Acids Res.* **2012**, *41* (D1), D955−D961.
(39) Xiao, H.; Zheng, Y.; Ma, L.; Tian, L.; Sun, Q. Clinically-Relevant ABC Transporter for Anti-Cancer Drug Resistance. *Front. Pharmacol.* **2021**, *12*, No. 648407.
(40) Fingar, D. C.; Salama, S.; Tsou, C.; Harlow, E.; Blenis, J. Mammalian Cell Size Is Controlled by MTOR and Its Downstream Targets S6K1 and 4EBP1/EIF4E. *Genes Dev.* **2002**, *16* (12), 1472−1487.
(41) Teng, T.; Mercer, C. A.; Hexley, P.; Thomas, G.; Fumagalli, S. Loss of Tumor Suppressor RPL5/RPL11 Does Not Induce Cell Cycle Arrest but Impedes Proliferation Due to Reduced Ribosome Content and Translation Capacity. *Mol. Cell. Biol.* **2013**, *33* (23), 4660−4671.
(42) Decker, T.; Hipp, S.; Ringshausen, I.; Bogner, C.; Oelsner, M.; Schneller, F.; Peschel, C. Rapamycin-Induced G1 Arrest in Cycling B-CLL Cells Is Associated with Reduced Expression of Cyclin D3, Cyclin E, Cyclin A, and Survivin. *Blood* **2003**, *101* (1), 278−285.
(43) Harley, M. E.; Allan, L. A.; Sanderson, H. S.; Clarke, P. R. Phosphorylation of Mcl-1 by CDK1−Cyclin B1 Initiates Its Cdc20-dependent Destruction during Mitotic Arrest. *EMBO J.* **2010**, *29* (14), 2407−2420.
(44) Ilık, İ. A.; Glažar, P.; Tse, K.; Brändl, B.; Meierhofer, D.; Müller, F. J.; Smith, Z. D.; Aktaş, T. Autonomous Transposons Tune Their Sequences to Ensure Somatic Suppression. *Nature* **2024**, *626* (8001), 1116−1124.
(45) Valgardsdottir, R.; Chiodi, I.; Giordano, M.; Rossi, A.; Bazzini, S.; Ghigna, C.; Riva, S.; Biamonti, G. Transcription of Satellite III Non-Coding RNAs Is a General Stress Response in Human Cells. *Nucleic Acids Res.* **2008**, *36* (2), 423−434.
(46) Yang, W.; Han, G. H.; Shin, H. Y.; Lee, E. J.; Cho, H.; Chay, D. B.; Kim, J. H. Combined Treatment with Modulated Electro-Hyperthermia and an Autophagy Inhibitor Effectively Inhibit Ovarian and Cervical Cancer Growth. *Int. J. Hyperthermia* **2019**, *36* (1), 9−20.
(47) Team, R. C. R: A Language and Environment for Statistical Computing. 2020.
(48) Kanda, Y. Investigation of the Freely Available Easy-to-Use Software 'EZR' for Medical Statistics. *Bone Marrow Transplant.* **2013**, *48* (3), 452−458.




https://doi.org/10.1021/acs.jmedchem.5c03361
J. Med. Chem. 2026, 69, 5944−5955